Environmental Sciences Europe

RESEARCH

Open Access

Integrated analysis of the occurrence and in situ sediment–water partitioning of selected pharmaceuticals in a riverine system

Aleksandër Peqini[1,2,4*], Benjamin Justus Heyde[1,3], Ferdi Brahushi[2] and Rolf-Alexander Düring[1,4]

Abstract

Twelve pharmaceuticals, including stimulant caffeine (CAFF), anti-inflammatories (naproxen (NPX), ibuprofen (IBU), and diclofenac (DCF)), antibiotics (anhydro-erythromycin (AETM), azithromycin (ATM), erythromycin (ETM), clindamycin (CMC), ciprofloxacin (CFC), sulfamethoxazole (SMX), and trimethoprim (TMP)), and the antiepileptic carbamazepine (CBZ), were analyzed in surface waters and sediments in the Ishmi River basin, Albania, across seasons during 2023 and 2024. This basin is characterized by limited wastewater treatment infrastructure, varying degrees of urban impact, and different environmental conditions. All targeted compounds were detected in water, with the highest concentrations observed near urban areas, particularly at the wastewater-impacted location LR1 for CAFF, IBU, NPX, and CFC with 22.5, 12.8, 2.7, and 1.8 µg L^{-1}, respectively. Sediment concentrations showed high levels of CFC and ATM, notably during spring with the highest concentrations of 1068 (LR1) and 396 ng g^{-1} (IR2), respectively, suggesting strong seasonal and spatial variability. Partitioning behavior (K_d and K_{oc}) was investigated in relation to compound-specific (D_{ow}) and sediment-specific (pH, organic carbon, $CaCO_3$ and metal content) properties. Significant correlations were found, and multiple regression models successfully predicted in situ K_d values for NPX, IBU, CFC, AETM, and CMC. These findings underline the influence of environmental and sediment characteristics on environmental pharmaceutical distribution.

Keywords Emerging contaminants, Sediment physico-chemical properties, D_{ow}, K_d modeling, Spatial–temporal pattern

Introduction

Pharmaceuticals are extensively used in treating humans or animal diseases because of their biological activity [26]. The global pharmaceutical market has expanded significantly over the past two decades; in 2019, its value reached approximately USD 1.25 trillion, compared to USD 390 billion in 2001 [16], indicating their increasing trend over the years. Pharmaceuticals may enter the environment through various pathways such as pharmaceutical factories and hospital effluents, household wastewater, livestock farm wastewater (feces and urine), wastewater treatment plant effluents, aquaculture, farmlands (sludge reuse as fertilizer), and solid waste disposal (unused and expired pharmaceuticals) [27], as well as wastewater irrigation [17]. In the environment,

*Correspondence:
Aleksandër Peqini
aleksander.peqini@umwelt.uni-giessen.de
[1] Institute of Soil Science and Soil Conservation, iFZ Research Centre for BioSystems, Land Use and Nutrition (iFZ), Justus Liebig University Giessen, Heinrich-Buff-Ring 26, 35392 Giessen, Germany
[2] Department of Environment and Natural Resources, Faculty of Agriculture and Environment, Agricultural University of Tirana, 1029 Tirana, Albania
[3] Present Address: Institute of Geography, Unit Soil Sciences and Soil Resources, Ruhr University Bochum, Bochum, Germany
[4] Kompetenzzentrum Wasser Hessen, Max-Von-Laue Straße 13, 60438 Frankfurt Am Main, Germany

pharmaceuticals are subject of abiotic and biotic processes such as biotransformation, biodegradation, photolysis, and sorption to suspended solids [3, 30]. The latter is getting more focus because of better assessment of their environmental behavior and potential effects on sediment-dwelling organisms. It is reported that the partitioning of pharmaceuticals is driven by the combination of physico-chemical properties of both compound and sediment [1, 49, 59]. At the same time, models considering these properties simultaneously are developed in order to predict their partitioning between environmental media [49]. But, as environmental conditions and certain site characteristics differ, these models still have weaknesses in predicting the distribution behavior of pharmaceuticals in the environment. Therefore, it is necessary to assess pharmaceutical partitioning through in situ developed models, considering the physico-chemical properties of the compounds and sediments under environmental conditions.

In this study, caffeine (CAFF), carbamazepine (CBZ), naproxen (NPX), ibuprofen (IBU), diclofenac (DCF), anhydro-erythromycin (AETM), azithromycin (ATM), erythromycin (ETM), clindamycin (CMC), ciprofloxacin (CFC), sulfamethoxazole (SMX), and trimethoprim (TMP) were chosen due to their environmental relevance and in the context of Albania's obligation, as a European Union (EU) candidate country, to align its water policies with the Water Framework Directive (Directive 2000/60/EC). This directive requires robust monitoring and reporting of water quality status across all water bodies. Based on the latest update of this directive watch list (Commission Implementing Decision (EU) 2025/439), only CMC remains in the watch list, due to insufficient monitoring data, while SMX and TMP were removed in 2024 (completed the four year monitoring cycle). Other compounds such as CBZ, IBU, DCF, ATM, ETM, and CFC (except CAFF, NPX and AETM) have been proposed for inclusion in the list of priority substances in surface waters. However, CAFF is particularly relevant to this study, as wastewater discharges into the Ishmi River are untreated and high CAFF inputs can therefore be assumed. NPX is the painkiller with the highest prescription rates in Albania. AETM as a transformation product of the antibiotic ETM frequently occurs in waste water and surface waters.

Pharmaceutical concentrations in aquatic environments typically range from below detection to the low μg L^{-1} level in developed countries [38, 42], while data from developing countries, such Albania in this case, remain limited. In this regard, there is only one study in Albania which detected only two compounds (caffeine at 45 ng L^{-1} and citalopram at 6–8 ng L^{-1}) in a northern Albanian River (Buna River) [57]. High concentrations of pharmaceuticals are found in lower-middle income countries due to increasing consumption of pharmaceuticals and limited wastewater treatment infrastructure [57].

Albania, classified as a middle-income country (World Bank, 2022), has over 30% of its population concentrated in the central-western region, where the Ishmi River is located. This area is notably lacking in functional wastewater treatment infrastructure, raising significant concerns regarding pharmaceutical contamination and broader environmental pollution. Albanian monthly average consumption data for 2023 and 2024 reported that CBZ, NPX, IBU, and DCF were used in quantities of 36.01 and 45.13 kg, 156.6 and 139.2 kg, 6.25 and 5.08 kg, and 0.82 and 0.85 kg, respectively. In contrast, the usage of antibiotics ATM, CFC, ETM, SMX, and TMP was considerably lower, with average monthly amounts of 0.05 and 0.02 kg, 0.60 and 0.56 kg, 0.08 and 0.09 kg, 0.47 and 0.58 kg, and 0.10 and 0.12 kg, respectively. Notably, AETM and CMC were not reimbursed during the reporting period. These values represent only the reimbursed quantities covered by the Mandatory Health Insurance Fund of Albania, accounting for an estimated 1–5% of total national pharmaceutical consumption. The study area lacks wastewater treatment, indicating high input of pharmaceuticals and that it is worthwhile investigating their partitioning behavior under environmental conditions. Therefore, the objective of this study was to assess the occurrence of the selected pharmaceuticals in water and sediments and their partitioning behavior by considering both compound properties and site-specific environmental conditions.

Materials and methods

Study area, sample collection and pretreatment

Sampling campaigns in the Ishmi River basin were carried out seasonally during 2023 and 2024 for surface water samples. For certain pharmaceuticals (AETM, ATM, CMC, CFC, ETM, SMX, and TMP), sampling was limited to three seasons, due to technical constraints in the analytical system, which prevented complete seasonal coverage for these compounds (Fig. 1; SM Table 1). Sediment samples were collected during the spring and summer seasons of both years (Fig. 1; SM Table 2). Site locations and brief site characteristics are summarized in Table 1. The Ishmi River basin includes several tributaries, such as the Tirana, Lana, Terkuzë, Gjoles, and Zeza Rivers, and discharges into the Adriatic Sea. The main stem of the Ishmi River spans 74 km, with the entire basin extending to approximately 152 km including its tributaries. Sampling sites were situated at established national water monitoring stations and categorized based on their relative position in the basin: upstream (Brari Bridge – TR1), midstream/urban areas (Casa Italia

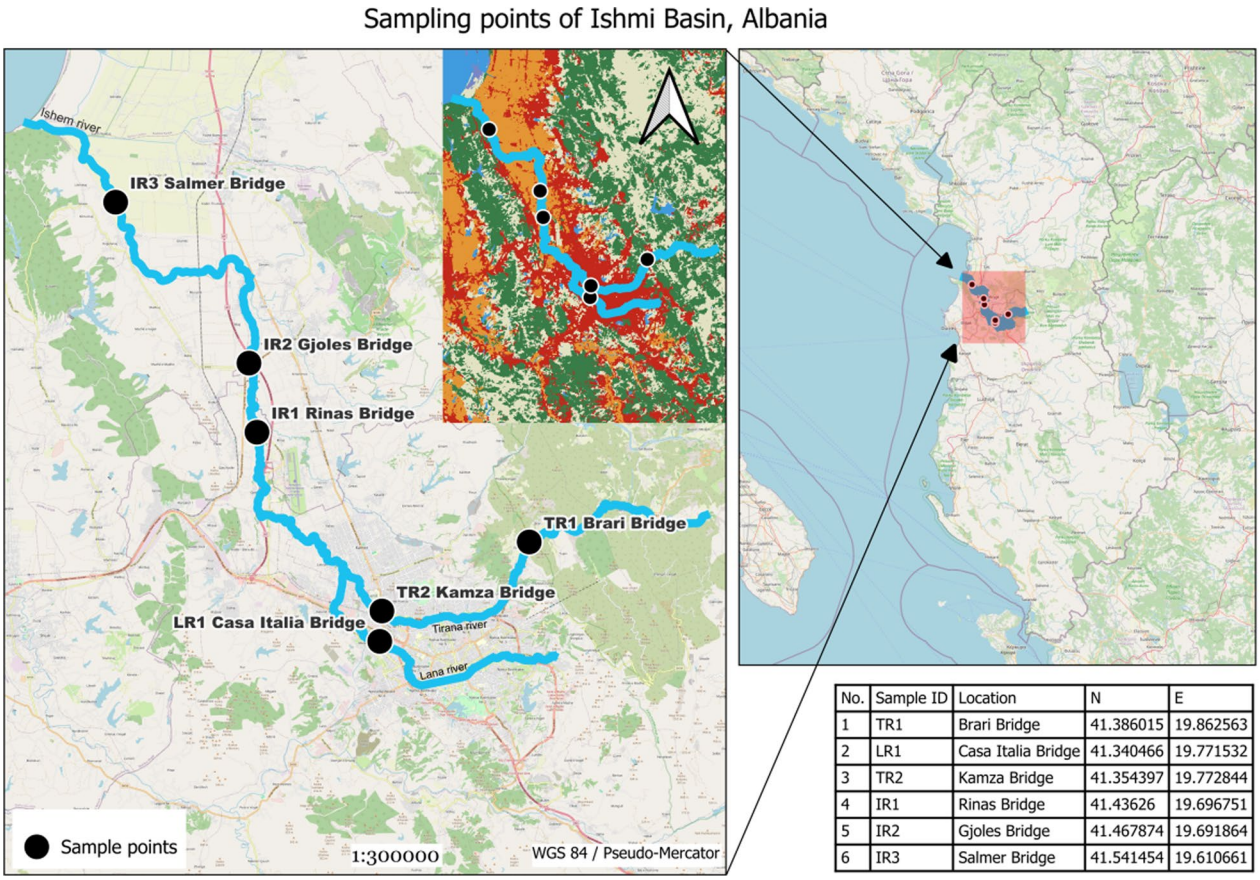

Fig. 1 Location of sampling points in the Ishmi River basin

Table 1 Sampled Ishmi basin Rivers sites characteristics

ID	River	Location	*Flow $m^3 s^{-1}$		Site characteristics
			Year 2023		
			Autumn	Summer	
TR1	Tirana River	N41° 38′; E19° 86′	0.31	0.55	Light human activity; touristic attraction
LR1	Lana River	N41° 34′; E19° 77′			Wastewater discharges and urban industry
TR2	Tirana River	N41° 35′; E19° 77′			Wastewater discharges and urban industry
IR1	Ishmi River	N41° 43′; E19° 69′			Wastewater discharges, agriculture, and urban industry; Tirana International Airport
IR2	Ishmi River	N41° 46′; E19° 69′			Urban and agriculture activities
IR3	Ishmi River	N41° 54′; E19° 61′	4.89	3.83	Agriculture activities

* Data from Report of Environmental State of the year 2023, National Environment Agency of Albania

Bridge – LR1, Kamza Bridge – TR2, Rinas Bridge – IR1), and downstream (Gjoles Bridge – IR2, Salmer Bridge – IR3). TR1 represented a site with minimal anthropogenic influence. In contrast, LR1, TR2, IR1, and IR2 were heavily impacted by urban activities, particularly LR1, and with some agricultural influence. IR3 was predominantly affected by agricultural activities (see Fig. 1, where red and orange indicate urban and agricultural land use, respectively).

The reported procedures to collect water and sediment samples were used [34, 39]. Surface water samples (grab samples) were collected in pre-cleaned (acetone and Milli-Q water) glass bottles. In the event of precipitation, sampling was delayed for approximately one week to

Table 2 Summary of mean concentrations of selected pharmaceuticals in the water and sediments of different locations from Ishmi River basin

Compounds	Water (ng L^{-1}) ($n=8$)						Sediment (ng g^{-1}) ($n=4$)					
	Sampling Point											
	TR1	LR1	TR2	IR1	IR2	IR3	TR1	LR1	TR2	IR1	IR2	IR3
CAFF	n.d	10,676	1,430	5,309	4,324	2,996	NM					
CBZ	41.1	260.5	n.d	21.7	28.2	n.d	2.5	44.1	15.2	9.7	11.5	9.6
NPX	n.d	2,028	525	1,255	914	585	2.8	18.4	5.6	8.8	4.8	1.6
IBU	n.d	11,297	1,037	8,384	7,926	1,450	n.d	47.2	8.3	16.0	8.0	9.0
DCF	n.d	278	n.d	47.5	50.2	59.6	NM					
AETM	10.7	26.5	6.0	32.3	10.8	58.2	0.3	0.9	0.9	0.7	0.9	0.6
ATM	n.d	1,501	n.d	n.d	n.d	n.d	n.d	113	54.0	122	16.0	48.2
CMC	5.2	12.3	23.3	36.7	20.2	9.8	11.8	8.1	3.8	4.3	4.6	17.8
CFC	179.2	714	404	407	188	348	3.2	705	77.9	170	129	48.6
ETM	n.d	n.d	230	24.3	n.d	n.d	*Added to AETM					
SMX	23.2	126	17.8	74.2	42.0	49.8	0.8	3.6	2.7	0.9	0.8	0.1
TMP	8.0	40.5	3.0	8.2	9.0	3.8	n.d	6.4	11.3	6.7	6.0	2.1

NM not measured, *Due to dominance of AETM, as dominant degradation product in acidic conditions

avoid dilution effects. Samples were immediately placed in a cooler, transported to the laboratory, and stored at 4 °C until extraction (within 48 h). Prior to extraction, samples were filtered using 0.45 µm cellulose acetate filters, and the filtrate pH was adjusted to 2.7 using concentrated HCl (37%).

Sediment samples were collected using a stainless steel stirring spatula (1 m length) from 0–5 cm depth, immediately cooled, and transported to the laboratory. Samples were frozen at − 28 °C and subsequently lyophilized. Dried sediments were homogenized using a mortar and pestle, sieved to < 100 µm, and stored at − 28 °C in glass containers until analysis. The processed sediment samples were analyzed for pH (the Association of German Agricultural Inspection and Research Insitutes (VDLUFA 1991) method was used), total nitrogen (TN) (the German Institute for Standardization (DIN EN 16168–2012-11) method was used), total hydrogen (TH), total sulfur (TS) (DIN ISO 15178:02–2001), total carbon (TOC) (DIN EN 15936:2012–11), carbonates ($CaCO_3$) (calculated from TOC and organic carbon), inorganic (IC) and organic carbon (OC) (VDLUFA (1991)), Al, Fe, Ca, K, Mg, Na (DIN ISO 11466/DIN EN 16174), and for the selected pharmaceutical concentrations based on reported validated methods [10, 34]. Sediment pH was determined in a 1:2.5 (w/v) suspension of sediment in 0.01 M $CaCl_2$, after shaking for 60 min at 150 rpm. The TN, TH, TS, and TOC were determined through thermal conductivity detection method with a CHNS elemental analyzer (UNICUBE®, Elementar, Langenselbold, Germany). Carbonates were determined with a Scheibler device, first dissolving the $CaCO_3$ with 10% HCl and then measuring the emitted CO_2. The IC was calculated by multiplying the carbonates with 0.1199 factor, while the OC was calculated by subtracting the carbonates from the TOC. Total metal concentrations were determined using inductively coupled plasma–optical emission spectrometry (ICP-OES, Varian 720-ES).

Chemicals

Pharmaceutical compounds were primarily selected based on their usage in Albania. Standards of CAFF, CBZ, NPX, IBU, and DCF were obtained from Sigma-Aldrich GmbH (Germany). Standard stock solutions (1000 mg L^{-1}) were prepared in methanol and stored at –20 °C. Working solutions were prepared monthly from the stock solutions. Antibiotic standards of AETM, ATM, CMC, CFC, ETM, SMX, and TMP, as well as internal standards, were purchased from HPC Standards GmbH (Cunnersdorf, Germany). Stock solutions of antibiotics were prepared in methanol containing 0.01% HCl. Organic solvents (acetone, methanol, and ACN, all HPLC grade) were obtained from VWR International (Radnor, PA, USA). Formic acid (99.6%) and sulfuric acid were obtained from VWR International (France). Potassium dihydrogen phosphate was purchased from Merck GmbH & Co. KG (Darmstadt, Germany). Orthophosphoric acid (H_3PO_4, 85%), hydrochloric acid (HCl, 37%), and ethylenediaminetetraacetic acid disodium salt dihydrate (EDTA, ≥ 99%) were purchased from Carl Roth GmbH & Co. KG (Karlsruhe, Germany). Membrane filters (cellulose acetate, 0.45 µm) and PTFE syringe filters

(0.45 µm) were obtained from OTTO E. KOBE KG (Marburg, Germany). C18-E (55 µm, 70 Å, 500 mg / 6 mL) Strata® cartridges were purchased from Phenomenex (USA). A Mettler Toledo balance (ME 204), Milli-Q water (18.2 MΩ·cm, Purelab, UK), and a pH meter (inoLab® pH 7110) were used throughout the study.

Water sample extraction

For the analysis CAFF, CBZ, NPX, IBU, and DCF, solid-phase extraction (SPE) was performed following the reported methods [39, 43]. The filtrate (500 mL, pH 2.7) was passed through C-18 SPE cartridges (Strata®, Phenomenex) via a Teflon tube at a flow rate of 3 mL min^{-1} by using an ISMATEC (ISM915A) peristaltic pump. Cartridges were pre-conditioned with 10 mL of acetonitrile (ACN) and 10 mL of acidified Milli-Q water (pH 2.7, adjusted with HCl) by using a 12-port vacuum manifold system (Macherey Nagel), connected to a vacuum pump. After extraction, analytes were eluted with a total of 14 mL of ACN: 2×5 mL under gravity flow and 4 mL of 0.1% HCl in ACN under vacuum. The combined solvent was evaporated to dryness under a gentle flow of nitrogen and reconstituted in 0.25 mL of 50:50 (v/v) ACN/Milli-Q water (pH 2.7), then filtered (0.45 µm PTFE) and measured using HPLC with UV and fluorescence detection (HPLC–UV/FLD) based on the reported method [33]. Meanwhile, AETM, ATM, CMC, CFC, ETM, SMX, and TMP were analyzed by direct injection (only filtered, pH-adjusted to 2.7, spiked with internal standards, and measured using high-performance liquid chromatography coupled with tandem mass spectrometry (HPLC–MS/MS) based on the reported method [10].

Sediment sample extraction

Sediment samples were analyzed for anti-inflammatories (NPX, IBU), the antiepileptic (CBZ), and selected antibiotics (AETM, ATM, CMC, CFC, SMX, TMP). CAFF and DCF were excluded from sediment analysis due to high matrix interference. For CBZ, NPX, and IBU, extraction was performed according to a previously reported method [34]. Briefly, replicate sediment samples (2 g) were treated with EDTA (0.2 g g^{-1} sediment) and subjected to a three-step extraction using 5 mL + 5 mL of methanol (0.1% formic acid), and 5 mL of acetone (0.1% formic acid), in 15 mL centrifuge tubes. Each step involved shaking at 350 rpm for 45 min, ultrasonication at room temperature for 30 min, and centrifugation at 3565 RCF for 20 min. The supernatants were combined and evaporated to dryness under a gentle nitrogen flow. The dried extracts were reconstituted in 0.22 mL of ACN, diluted to 250 mL with Milli-Q water acidified to pH 2 (50% H_2SO_4), passed through C18 SPE cartridges, and processed as the water extraction procedure above. Standard addition was performed using 0.5, 1.0, and 2.5 mg L^{-1} for calibration. Both unspiked and spiked samples were analyzed using HPLC–UV/FLD based on the reported method [33].

For AETM, ATM, CMC, CFC, SMX, and TMP (with ETM included in AETM), the extraction followed a previously published method [10]. Shortly, replicate sediment samples (2 g) were extracted with 26 mL of 0.2 M KH_2PO_4:ACN (1:1, v/v) in 50 mL glass vials. An aliquot (1 mL) of the extract was evaporated under nitrogen, reconstituted in 1 mL of 50 mM H_3PO_4:ACN (80:20, v/v), spiked with internal standards, and analyzed by HPLC–MS/MS based on the reported method [10].

Determination of pharmaceuticals

Compounds with available isotopically labeled internal standards were analyzed by LC–MS/MS, while others were quantified using HPLC–UV/FLD with standard addition to correct for matrix effects, thus ensuring reliable results while balancing analytical feasibility and costs.

An analytical method previously reported for the determination of CAFF, CBZ, NPX, IBU, and DCF was applied [33]. Briefly, compounds were analyzed by liquid chromatography using an Agilent 1200 HPLC system (Agilent Technologies Inc., USA) equipped with a column oven (G1316A), autosampler (G1329A), quaternary pump (G1311A), diode array detector (DAD, G1315B), and fluorescence detector (FLD). Separation was performed on a reverse-phase C18 column (3 µm, 120 Å, 2.1×150 mm). The DAD was set at 285 nm for CAFF and CBZ, and 220 nm for IBU and DCF. NPX was detected using the FLD, with excitation and emission wavelengths of 230 nm and 420 nm, respectively. Chromatographic separation was achieved within 57 min using a mobile phase consisting of ACN containing 0.5% H_2O (solvent A) and a 25 mM potassium dihydrogen phosphate buffer at pH 2.7 (solvent B). The gradient program was as follows: 15% A (0–4.5 min), 20% A (4.5–12.5 min), 25% A (12.5–18 min), 45% A (18–38 min), 80% A (38–45 min), and re-equilibration at 15% A (45–57 min). The column temperature was maintained at 40 °C, with an injection volume of 20 µL and a flow rate of 0.3 mL min^{-1}. Instrument control, data acquisition, and processing were performed using ChemStation software. The limits of quantification (LOQs) were established from matrix-matched SPE calibrations in Ishmi River water (IR1). Calibration curves were prepared by spiking IR1 and Milli-Q water (0.1–10 µg L^{-1}) and processing 500 mL samples through SPE (0.25 mL final extract). LOQs (ng L^{-1}) were 2.3 (CAFF), 97.0 (CBZ), 30.5 (NPX), 42.4 (IBU), and 188.6 (DCF). Based on these values, sediment-equivalent LOQs were derived according to the ratio of extract volume to sediment mass. Quantification was performed by

standard addition to multiple sample aliquots to correct for matrix effects; although the formal LOQs were established from the validated calibration range (12.1 ng g^{-1} for CBZ, 3.8 ng g^{-1} for NPX, and 5.3 ng g^{-1} for IBU), signals below these levels were occasionally visible due to the enhanced sensitivity of the standard addition approach. Recoveries (%) in water (IR1water spiked at 2 µg L^{-1}) were 24.4 (CAFF), 111.7 (CBZ), 107.6 (NPX), 108.8 (IBU), and 108.4 (DCF), while in sediments (IR1 sediment spiked at 300 ng g^{-1}) they were 92.8 (CBZ), 83.6 (NPX), and 92.9 (IBU).

For AETM, ATM, CMC, CFC, ETM, SMX, and TMP the reported analytical method was applied [10]. Analyses were performed with a Sciex™ ExionLC™ separations module, equipped with an auto sampler unit, a gradient pump, a column oven and a sample heater. The chromatographic device was connected via Peek capillary (0.18 mm ID) to a Sciex™ triple quadrupole mass spectrometer (QTRAP 4500™). The method used a Waters Bridge™ C18 Column (150 mm length, 2.1 mm ID, 3.5 µm particle size) and a column guard of the same material. Eluents were A: Milli-Q-water (0.1% formic acid) and B: ACN (0.1% formic acid). The flow was 0.4 mL min^{-1} and the sample cooler was set to 20 °C. The MS–MS measurement was performed in positive mode with 2500 V on the source capillary and 500 °C desolvation temperature. Nitrogen was used as curtain and collision gas (further MS parameters are provided in SM Table 3). The LOQs in µg L^{-1} for the analyzed antibiotics were as follows: 0.01 (SMX), 0.09 (TMP), 0.12 (CFC), 0.02 (CMC), 0.16 (AETM/ETM), and 0.47 (ATM). The corresponding LOQs in µg kg^{-1} were 0.01 (SMX), 0.09 (TMP), 0.12 (CFC), 0.02 (CMC), 0.16 (AETM/ETM), and 0.47 (ATM). Isotope-labeled internal standards were applied during measurement to ensure data integrity and analytical quality. The standards used were SMX-$^{13}C_6$, CMC-$^{13}Cd_6$, ATM-$^{13}Cd_3$, CFC-d_8, and TMP-d_9, each assigned to its corresponding analyte. For ETM, TMP-d_9 was used as a class-matched surrogate standard. LOQ values were determined as the mean concentrations measured in blank samples plus five times their standard deviation. When the calculated LOQ was lower than the lowest calibration level, one-half of the lowest calibration concentration was adopted as the LOQ. Extraction recoveries of the sediments extraction method varied between 50–120% for antibiotics. LC–MS/MS recovery in water samples was not tested separately, but internal standards were used to calculate the matrix effect and monitor the analytical process. If the recovered signal deviates significantly (50–120%) from the expected signal, this is considered a trigger.

Data treatment

The sediment–water partition coefficient (K_d) for the selected pharmaceuticals was calculated using their concentrations in the sediment phase (C_s) (ng g^{-1}) and the water phase (C_w) (ng L^{-1}), according to Eq. (1), as reported by [44].

This coefficient is considered as one of the key factors influencing the persistence and long-term fate of contaminants in aquatic environments. A higher K_d value indicates greater sorption to sediments, suggesting stronger binding and higher environmental persistence due to reduced photodegradation and biodegradation processes [7].

$$K_d = C_s / C_w \tag{1}$$

Another parameter that describes the distribution of a compound between water and sediment is the pH-dependent *n*-octanol–water partition coefficient (D_{ow}). This parameter accounts for the compound's ionization at a given pH. To assess the distribution behavior of the selected pharmaceuticals, D_{ow} was calculated using Eq. (2), as reported by [54].

Table 3 K_d and K_{oc} calculated values on site compared with literature values

Compound	K_d (mL g^{-1})			K_{oc} (mL g^{-1})			Literature (mL g^{-1})		Matrix	References
	Min	Max	Mean	Min	Max	Mean	K_d	K_{oc}		
ATM	369.2			3,144.7			121–1,834	17,783	Sediment	[29, 44]
AETM	12.5	178.1	114.2	678.8	4,340.5	2,699.7	2–73; 211	–	Sediment	[44, 47]
CFC	13.9	8534.4	2,180.9	828.8	135,037	42,472.9	329.3–4,664	–	Sediment	[59]
CMC	3.06	971.2	224.0	132.8	157,148	24,276	0.7–570	125.9–25,119	Sediment	[29]
IBU	0.17	27.3	9.09	7.49	784.9	236.4	1.72–45.5	192–1,110	Soil	[56]
NPX	0.42	24.8	8.10	10.91	762.9	209.7	3.4–356	340–7,610	Soil	[56]
SMX	54.2	197.3	115.5	623.3	4,555.6	3,117.6	22–105	–	Sediment	[18]
TMP	39.3	3,142	720.5	1,076.9	4,9726	12,854	18.8–3,126	–	Sediment	[18, 49]

$$D_{ow} = \frac{K_{ow}}{1 + (10^{pH - pK_a})} \quad (2)$$

where K_{ow} is the *n*-octanol–water partition coefficient and pK_a is the acid dissociation constant.

The organic carbon content in sediments significantly influences the distribution of organic compounds between the water and sediment phases. Organic carbon provides abundant adsorption sites and facilitates hydrophobic interactions, enhancing the sorption of both polar and non polar compounds. To evaluate this influence, the organic carbon-normalized partition coefficient (K_{oc}) was calculated using the Eq. (3), as reported by [56].

$$K_{oc} = K_d / f_{oc} \quad (3)$$

where f_{oc} represents the fraction of organic carbon.

Statistical analysis

For CAFF, CBZ, NPX, IBU, and DCF in water samples, statistical analysis was not performed due to limited sample volume and lack of replication. Instead, concentration data were summarized descriptively to illustrate spatial and seasonal patterns. In contrast, for sediment samples, the remaining pharmaceuticals in water samples, and the total concentrations across water and sediment phases, a two-way analysis of variance (ANOVA) was conducted. Season and location were considered as independent variables, while pharmaceutical concentration served as the dependent variable. When the assumptions of ANOVA (normality and homogeneity of variances) were not met, non-parametric Kruskal–Wallis tests were applied as an alternative. In addition, single and multiple stepwise regression analyses were used to examine relationships between the calculated distribution coefficient (K_d) and sediment properties, as well as with the predicted K_d. Statistical significance was set at $p < 0.05$. All analyses were performed using OriginPro 2015 (OriginLab Corporation, USA).

Results and discussion

Occurrence of the studied pharmaceuticals in surface waters and sediments

A summary of mean values of selected pharmaceuticals detected in water and sediment samples from the Ishmi River basin is presented in Table 2. Full datasets of concentrations in surface water samples at each sampling location and during seasons of 2023 and 2024 are shown in SM Table 1. All 12 investigated pharmaceuticals were detected. In general, the highest concentrations were observed at location LR1, in line with urban impact, then a decreasing trend with lowering the urban impact was observed, while concentrations at TR1 were typically low or below detection limits. CAFF, IBU, NPX, and CFC exhibited the highest environmental concentrations at almost all locations (except TR1), significantly at location LR1 with mean concentrations of 10.7, 11.3, 2, and 0.7 μg L^{-1}, respectively. CAFF is considered as one of the water treatment tracers [11], due to its limited use only to humans and high removal rates mainly during the biological treatment at the wastewater treatment plants [60]. In the continent of Europe (where Albania is part of), daily intake of CAFF was reported at 288.58 mg/person/day [24], although Albania encourages pregnant and lactating women to reduce CAFF product consumption (≤200–300 mg caffeine/day), and discourages CAFF containing products intake from childrens [41], the detected concentrations were up to 22.5 μg L^{-1} (considering a comparably low recovery rate of 24.4%), comparing only to urban impacted waters and wastewater influent concentrations such as in Brazil, in Portugal, and Hungary with 16.5, 9.4–83.9, and 221.4 μg L^{-1}, respectively [11, 22, 37]. Anti-infammatories such as IBU and NPX, were also detected in relatively high concentrations, especially at location LR1, with maximum of 12.8 and 2.6 μg L^{-1}, respectively. DCF was also detected, with the highest concentration of 1.8 μg L^{-1}at the same location, but lower frequency was observed compared to IBU and NPX. Under environmental surface water pH > 6, IBU, NPX, and DCF exist as ionized molecules, due to their pK_a values of 4.9, 4.2, and 4.5, respectively. Therefore, these compounds tend to remain in the aqueous phase. These concentrations are in agreement with those reported in the Turia River in Valencia [5], where the highest concentrations for IBU, NPX, and DCF were 7.2, 6.6, and 3.5 μg L^{-1}, respectively. The antiepileptic CBZ concentrations ranged from n.d. to 1.3 μg L^{-1} as maximum value at location LR1. This compound is relatively stable under environmental conditions, but the detection frequency was not consistent along all sites, possibly due to dilution from basin tributaries in the downstream locations (after LR1). Similar patterns are reported from Lis River, Portugal [38] and in the main Rivers of Madrid, Spain [51]. The fluoroquinolone CFC, similarly, to CAFF, IBU, and NPX, showed high frequency and relatively high concentrations, with a maximum of 1.8 μg L^{-1} again at location LR1. This compound is characterized by a low Henry's constant (< 10^{-15} atm*m^3 mol^{-1}) and, at pH values of 6.1–8.7 in the sediment samples, behaves mainly as zwitterionic but could also be positively or negatively charged (pK_a of 6.09 and 8.76), therefore it remains in aqueous phase [52]. CFC levels were comparable to those reported in studies in River waters and wastewater effluents such as in Iran (0.2–0.7 μg L^{-1}) [35], in Portugal (0.2–0.5 μg L^{-1}), in Spain (0.2 μg L^{-1}), in Ireland (0.2–0.3 μg L^{-1}), in Cyprus (0.3 μg L^{-1}), in Germany (0.2 μg L^{-1}), and in Norway (0.2 μg L^{-1}) [42]. Macrolides such as AETM, ATM, ETM,

and CMC, were also detected but showed different patterns. AETM and CMC were more frequently detected with levels ranging from n.d.–0.3 to n.d.–0.2 μg L^{-1}, respectively. ETM, is reported to be unstable and has a fast conversion rate to AETM [46]. Our results are in line with this behavior as ETM was detected only in two locations with 0.2 μg $L^{-1}$and 1.4 μg L^{-1}, similarly to trends reported in China (0.2 μg L^{-1}) [19] and in Spain (0.3–3.9 μg L^{-1}) [40, 51]. ATM was frequently detected only at location LR1, with the highest concentration of 7.5 μg L^{-1}. This pattern indicates that the main source of ATM was from high urban input and a relatively higher resistance to biodegradation [46, 55]. The sulfonamide SMX and diaminopyrimidine TMP exhibited high frequency with the highest concentrations registered at location LR1 with 0.4 μg L^{-1} and 0.1 μg L^{-1}, respectively, which are comparable with concentrations of 0.2 μg L^{-1} (SMX) and 0.3 μg L^{-1} (TMP) reported in surface waters [36].

For sediments, concentrations of selected pharmaceuticals in sediment samples at each sampling location during seasons of the years 2023 and 2024 are given in SM Table 2. Compared to water sample trends, CFC and ATM were detected in significantly higher concentrations during spring seasons ($p < 0.05 - 0.001$), with maximum of 1068 and 396 ng g^{-1}, respectively, followed by IBU (93.7 ng g^{-1}) > CBZ (60.5 ng g^{-1}) > NPX (49.3 ng g^{-1}) > TMP (38.3 ng g^{-1}) > CMC (37.8 ng g^{-1}) > SMX (13.3 ng g^{-1}) > AETM (2.7 ng g^{-1}). Similarly to water samples pattern, location LR1 showed a detection frequency of 100% for most compounds (except AETM and SMX with 50%), indicating that high input from urban discharge is the main source of contaminants in the surface waters. Under similar environment and anthropogenic impact conditions, maximum concentrations for CFC are reported at 1287 ng g^{-1} [62], for ATM at 8.1–14,680 ng g^{-1} [46], for IBU, CBZ, NPX at 66–340, 38–519, 3–96 ng g^{-1}, respectively [6], for TMP at 11–90 ng g^{-1} [20], for CMC at 87.7 ng g^{-1} [25], for SMX at 10 ng g^{-1} [2], and for AETM at 0.86–185 ng g^{-1} [46].

Partitioning of the studied pharmaceuticals in the sediment–water system

Having the concentrations of both aqueous and sediment phases, in situ K_d values of pharmaceuticals were calculated and the minimum, maximum, and the mean values, as well as all in situ calculated K_d values, are presented in Table 3 and SM Table 6, respectively. The K_d values varied highly for most of the compounds, as from 0.42 to 24.8 mL g^{-1} for NPX, from 0.17 to 27.3 mL g^{-1} for IBU, from 12.5 to 178.1 mL g^{-1} for AETM, from 3.06 to 971 mL g^{-1} for CMC, from 13.9 to 8534 mL g^{-1} for CFC, from 54.2 to 197 mL g^{-1} for SMX, and from 39.3 to 3,142 mL g^{-1} for TMP. For all compounds, similar trends were reported in the literature under comparable conditions, with wastewater discharge concluded as predominant factor (Table 3) [18, 29, 44, 47, 49, 56, 59]. The K_d is a very important parameter for understanding not only the behavior and matrix affinity of pharmaceuticals, but also for uptake and sorption mechanisms from sediments, through multiple linear correlations mainly with pH, OC (%), D_{ow}, cation exchange capacity (CEC), clay content (%), and selected sediment cations content (Al, Fe, K, Ca, Mg, Na), as reported in similar studies [1, 49, 59]. In this study, the calculated K_d of both detected water and sediment compounds, was correlated with sediment pH, OC (%), calculated D_{ow}, $CaCO_3$, and total content of selected sediment cations (Al, Fe, K, Ca, Mg, Na) in single and multiple linear regressions, with respective data given in SM Table 7 and SM Table 8, respectively. From the single linear correlations, it was observed that sediment pH, D_{ow}, and OC content had the highest impact on selected pharmaceuticals partitioning.

Of the seven compounds of which K_d was calculated, only five (NPX, IBU, AETM, CFC, CMC) were included in the multiple linear regression modeling. This judgement was based on the statistical significance of correlations and the ability to generate robust regression models with acceptable Adj. R^2 and root mean square error (RMSE) values (Fig. 2). SMX and TMP were excluded as they did not meet the criteria for reliable model development, due to weak or non-significant relationships with the sediment properties. Based on developed models of NPX, IBU, AETM, CFC, and CMC, their respective predicted values of K_d at all locations and seasons, and graphs with linear fittings are presented in SM Table 9 and Fig. 2, respectively. From the models and the fittings data, it could be observed that for CFC, NPX, and IBU the models were accurate and could be used to predict their environmental concentrations. Meanwhile, AETM and CMC, although showing good fitting relationship between calculated and predicted values (especially for AETM), the significance was not achieved during the multiple step fitting analysis.

The calculated D_{ow} values of each compound at each sediment pH showed a significant relationship with the increase of OC (SM Fig. 1). The K_{oc} values also varied from 10.9 to 763 mL g^{-1} C for NPX, from 7.5 to 785 mL g^{-1} C for IBU, from 679 to 4,341 mL g^{-1} C for AETM, from 133 to 157,148 mL g^{-1} C for CMC, from 829 to 135,037 mL g^{-1} C for CFC, from 623 to 4,556 mL g^{-1} C for SMX, and from 1,077 to 49,727 mL g^{-1} C for TMP.

The effect of sediment properties on selected pharmaceutical distribution in sediments

In general, sorption of pharmaceuticals in sediments is influenced by the physico-chemical properties of the

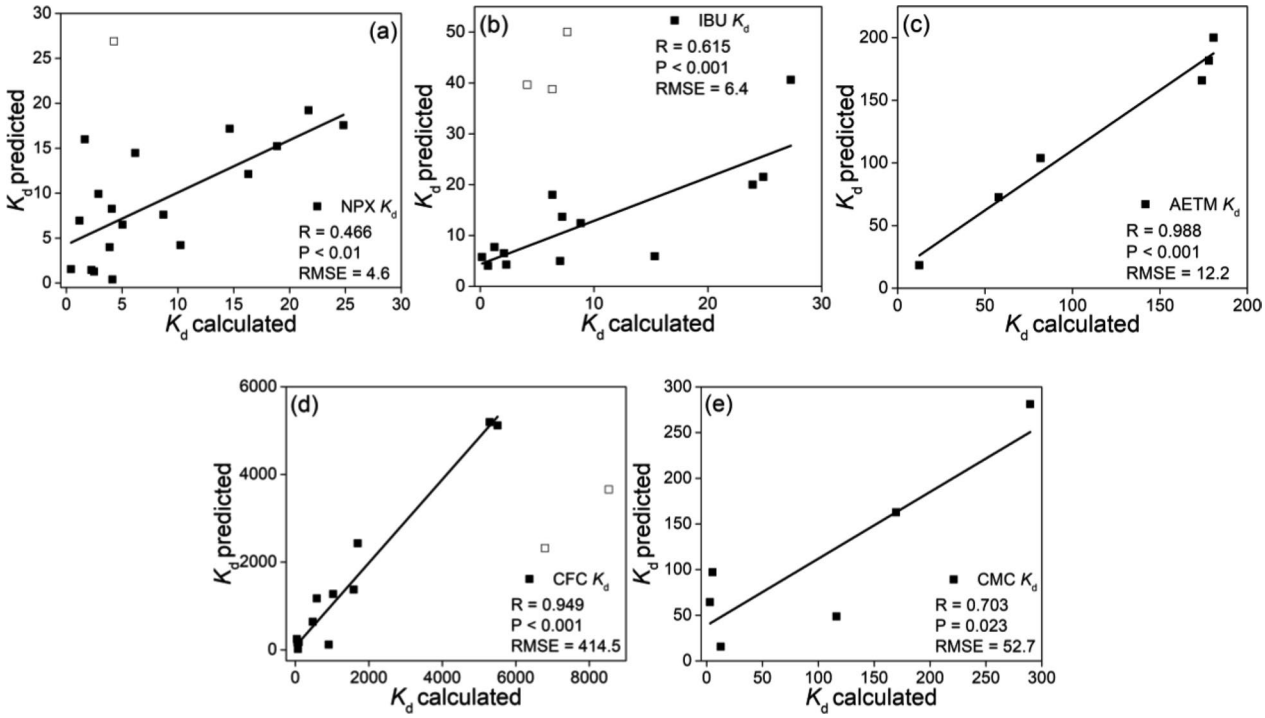

Fig. 2 The relation (model validation) between the calculated and predicted K_d of (**a**) NPX; (**b**) IBU; (**c**) AETM; (**d**) CFC; and (**e**) CMC

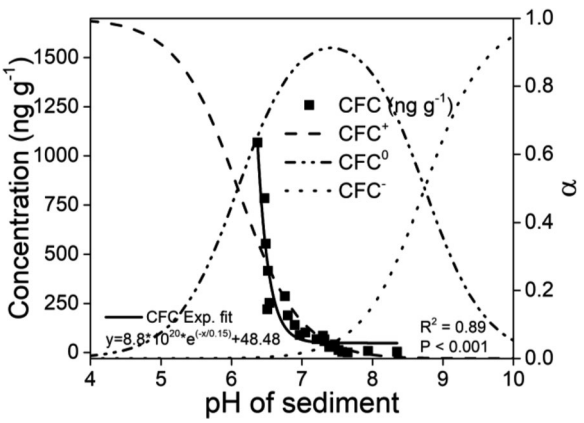

Fig. 3 The effect of sediment pH on CFC detected concentrations in sediments

compounds (hydrophobicity and chemical charge) as well as the properties of the sediment itself, mainly, OC content, CEC, cation content, and surface charge [15, 18]. These factors (including compounds properties) are all pH-dependent. At first, the effect of sediment pH on CFC concentrations in sediments followed an exponential trend, highlighting the prominent role of pH (Fig. 3).

Apart from influencing the compound speciation, sediment pH also governs the surface charge of sediments. As sediment pH increases, the net negative charge of the sediment also increases due to the deprotonation of surface functional groups (–OH) [4]. To evaluate the isolated effect of sediment pH on each pharmaceutical detected in the sediment phase, taking into account compound speciation, the corresponding data are presented in SM Fig. 3. The observed effect of sediment pH on compound concentrations was consistent with trends in the calculated distribution coefficient D_{ow} for most compounds (except CBZ which remains neutral under environment pH). Under these conditions, hydrophobic partitioning (K_{ow}) alone is not sufficient to assess the sorption behavior of pharmaceuticals in sediments due to their polar functional groups and their ionic nature [58]. For the selected pharmaceuticals, a significant negative relationship was observed between log K_{ow} and log K_{oc}, suggesting that compounds with higher hydrophobicity exhibited lower affinity for sediment organic matter, potentially due to other physico-chemical interactions influencing their sorption behavior (Fig. 4a). In addition to hydrophobic interactions, pharmaceutical sorption is largely driven by ionic interactions, which are pH dependent [50]. Therefore, their sorption assessment should not consider only K_{ow} but also the D_{ow}, which accounts for compound ionization at environmental pH. The calculated D_{ow} (using sediments pH) for each compound,

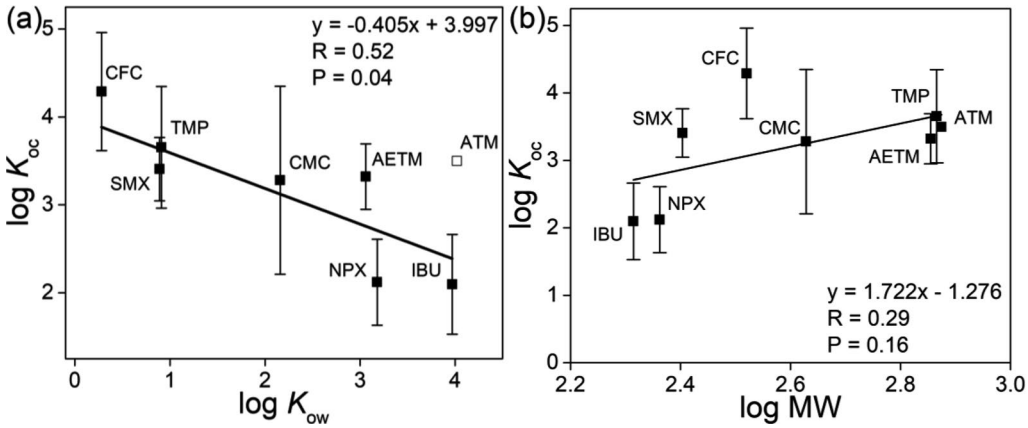

Fig. 4 (**a**) Relationship between the calculated log K_{oc} with log K_{ow} and (**b**) with log MW of the selected pharmaceuticals

showed an exponential decrease with increasing sediment pH, indicating a strong influence of pH on the ionic state of the compounds (SM Fig. 2). The molecular weight (MW) of the pharmaceuticals appeared to influence their presence in sediments. Although the relationship was not statistically significant, a positive linear trend between log K_{oc} and log MW was observed (Fig. 4b), which is consistent with findings from previous studies [7, 61].

Another important factor influencing the uptake of organic compounds in sediments is the OC content, which showed a significant positive linear correlation with the calculated D_{ow} values of the compounds (SM Fig. 1). Accordingly, by considering the physicochemical properties of pharmaceuticals, such as pK_a (SM Table 4), the relationship between calculated log K_{oc} and compound speciation (α, derived using Henderson-Hasselbalch equation) with sediment pH was examined for NPX, IBU, AETM, CMC, CFC, TMP, and SMX (both detected sediment and water matrix compounds, sampled at each time), and shown in Fig. 5a-g. In addition, based on data from both sediment and water phases under environmental sediment conditions (Table 3), sediment properties (SM Table 5), as well as their impact (SM Table 7), certain sorption trends can be identified.

The antiepileptic CBZ was detected mainly in sediment samples, indicating a higher affinity for sediments rather than waters. This pattern may be attributed to its environment persistence [38], resulting in an accumulation in the sediment over time. CBZ has a low K_{ow} and a relatively high water solubility but is not ionizable at water pH (pK_a 13.9) [54]. Therefore, the uptake mechanism is mainly through hydrophobic interactions between CBZ benzene rings and the hydrophobic organic carbon fractions of the sediments [32, 48], confirmed in this study with the fact that higher CBZ concentrations were detected at location LR1 where its content is the highest (OC ≈ 10%) (SM Fig. 1).

Anti-inflammatories such as NPX and IBU exhibited higher affinity for water compared to sediments, likely due to their acidic nature and predominant anionic speciation within the environmental pH range (6.4–8.4). Sorption of both compounds increased at lower sediment pH, with a decreasing trend observed as pH increased (Fig. 5a, b). As sediment pH increased, NPX ($pK_a = 4.2$) and IBU ($pK_a = 4.9$) exist predominantly in anionic forms, resulting in reduced sorption due to enhanced electrostatic repulsion with negatively charged sediment sites. This is supported by the significant negative correlations between K_d values and both pH and D_{ow} (SM Table 7). K_d values showed a significant positive correlation with Al ($p < 0.05$) and positive, though not statistically significant, correlations with OC, Fe, K, and Na. These findings indicate that NPX and IBU sorption under the studied pH conditions is primarily driven by electrostatic interactions between their deprotonated carboxylic groups and positively charged mineral oxide surfaces (Al, Fe, K, Na) and protonated amines of sediment organic matter [56].

Macrolides, such as AETM, ATM, and CMC, especially ATM, showed a higher affinity for sediments than for the aqueous phase. Within the studied sediment pH range (6.4–8.4), ATM ($pK_a = 8.7$) existed mainly in its protonated form, and the higher sorption was under low pH values (≈6.5) (SM Fig. 3e). The higher prevalence of ATM can be related with its higher biodegradation resistance [55] compared to AETM and CMC, and higher electrostatic interactions due to the presence of basic amine-N ligands (positively charged) of ATM with the negatively charged sites of the sediments, mainly of organic matter [46]. AETM (including ETM) also existed mainly in its cationic form ($AETM^+$) within this pH range (Fig. 5c).

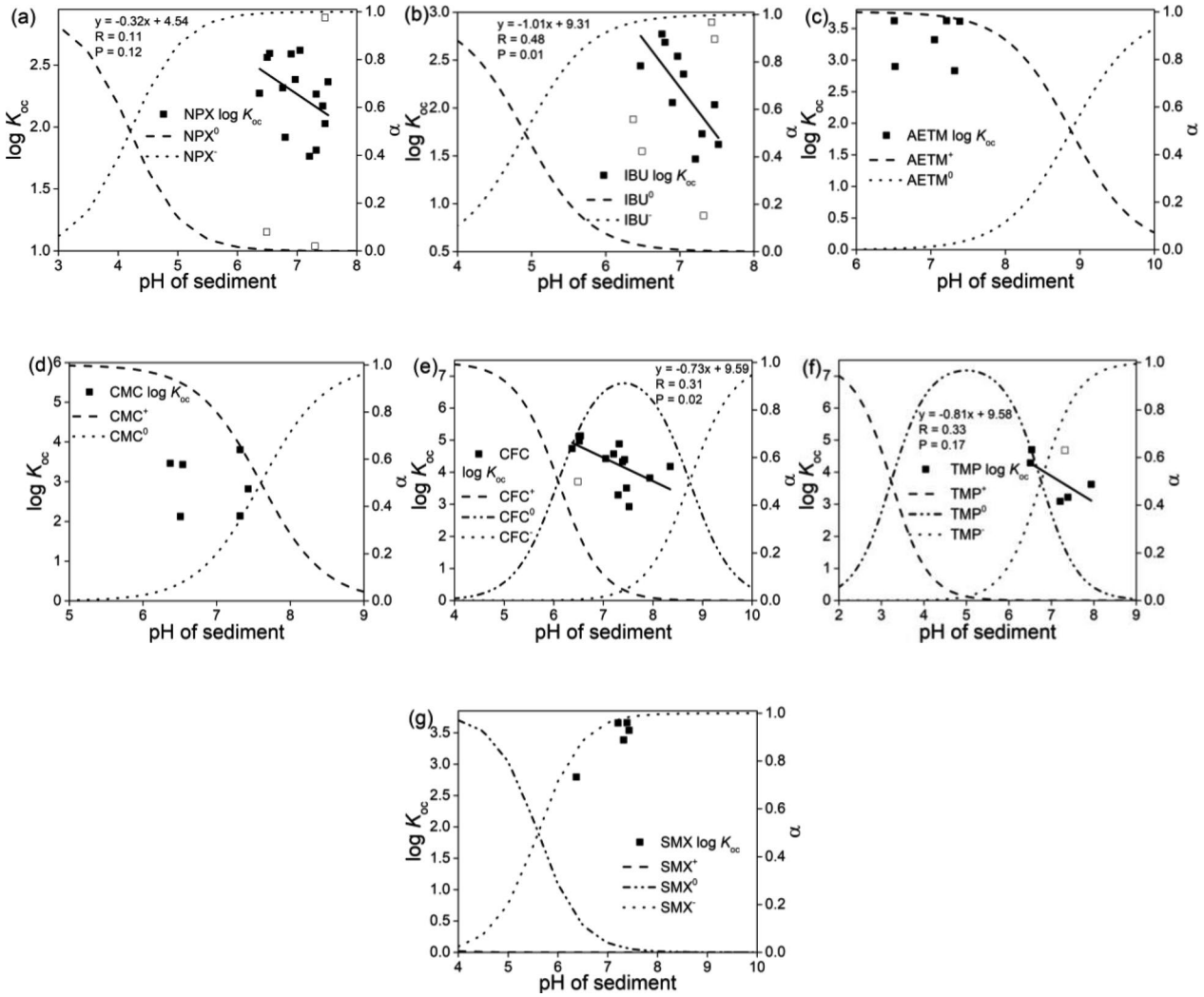

Fig. 5 The effect of sediment pH on log K_{oc} of (**a**) NPX; (**b**) IBU; (**c**) AETM; (**d**) CMC; (**e**) CFC; (**f**) TMP; and (**g**) SMX

Sorption of AETM was driven by electrostatic attraction to negatively charged functional groups of sediment organic matter and hydrogen bonding [12, 31], as can be seen from the significant positive correlation of K_d with OC and the negative correlation with sediment pH, D_{ow}, and other parameters including $CaCO_3$, Al ($p < 0.05$), Fe, Ca, K, Mg ($p < 0.05$), and Na ($p < 0.05$) (SM Table 7). CMC, with a pK_a of 7.6, in the pH range (6.4–8.4) of the studied sediments, existed predominantly in its cationic form (CMC^+) at pH values under 7.6, and mostly in its neutral form (CMC^0) at pH values above 7.6 (Fig. 5d). Generally, CMC was detected mostly and slightly in higher concentrations in sediments with a pH lower than 7, after which a decreasing trend was observed (SM Fig. 3f). Considering the negatively charged sediments, and predominantly occurring cationic CMC^+, cation-exchange is the responsible mechanism for CMC uptake from sediments, as reported under similar pH conditions [21, 45]. This is further supported by its similar K_d behavior to AETM with respect to sediment properties (SM Table 7).

The fluoroquinolone CFC, has two pK_a values (6.09 and 8.76) and within the relevant pH (6.4–8.4) of the sediments of the current study, can be mainly zwitterionic but at the same time, can be charged positively, negatively, or uncharged (Fig. 5e). The highest CFC concentrations were achieved at the lowest pH values (≈6.4) and with high OC of sediments (≈ 10%), then a decreasing trend in CFC was observed at higher sediment pH locations (electrostatic repulsion with the increase of CFC^-). Interestingly, the increase of sediment pH resulted in a significant exponential decrease of CFC sediment concentrations (Fig. 3), thus confirming that the sediment CFC uptake mechanism is through electrostatic

interactions between cationic CFC^+ with sediment surface negatively charged sediment functional groups, such as –OH, –COOH (OC, $p < 0.05$), C–O, and Si–O–Si [23, 53]. This is supported by the fact that the detected concentrations are similar to the percentage of CFC^+ (Fig. 3), and a significant negative correlation of CFC K_d with sediment pH and D_{ow} ($p < 0.001$) (SM Table 7). In addition, CFC K_d showed negative correlation with $CaCO_3$, Al, Fe ($p < 0.05$), Ca ($p < 0.05$), K ($p < 0.05$), Mg ($p < 0.05$), and Na, thus neutralizing sediment negative charges, resulting in an inhibitory effect on CFC sorption [23].

Diaminopyrimidines, such as TMP, though in lower concentrations show a higher affinity for sediments. TMP has two pK_a values (3.23 and 6.76), and can be zwitterionic (pH < 6.76) or negatively charged (pH > 6.76) under the sediment pH values of this study. The highest TMP sorption to sediments was observed at around pH 6.4 and with high OC content (positive correlation of TMP K_d with OC), suggesting hydrophobic interactions as the main sorption mechanism (SM Table 7 and Fig. 5f), as reported in a similar study with sediments [28]. With the increase in sediment pH, a decrease in TMP sorption was observed, due to the progressively increasing anionic TMP^- (pH > pK_a = 6.76) and the negative net charge of sediments, thus decreasing hydrophobic partitioning. Under these conditions, TMP uptake mechanism into the sediment is through electrostatic interactions, possibly between positively charged sites of sediment aluminium oxides with the anionic TMP^-, supported by the positive correlation of TMP K_d with sediment Al content [28, 56].

Sulfonamides, such as SMX, showed a higher tendency for the aqueous phase than for sediments, although low concentrations have also been detected in sediments (0.4 – 13.3 ng g^{-1}). Within the pH range of the studied sediments (6.4–8.4), SMX mainly exists in its anionic form (SMX^-), due to its low pK_a values (1.7, 5.6, and 5.9). Under these conditions, the affinity of sediments for SMX^- is not that high (electrostatic repulsion) as would be for SMX^0 (hydrophobic interactions), and the mechanism of sorption to the sediments, is by cation bridging between SMX^- with aluminium and iron oxides (SMX K_d positively correlated with Al and Fe sediment content, SM Table 7), and minor contributions from van der Waals forces [8].

Spatial and seasonal variations

Total concentrations of the selected pharmaceuticals for each sampled season in 2023 and 2024, in both water and sediment phases, are presented in SM Fig. 4 and in Fig. 6, respectively. The effects of location and season on the distribution of selected pharmaceuticals in both water and sediment phases of the basin were assessed using two-way ANOVA and non-parametric Kruskal–Wallis tests, with the results presented in SM Tables 10 and 11, respectively.

For waters, concentrations of selected pharmaceuticals varied significantly across sampling locations and seasons. Overall, levels were highest at LR1, followed by a decreasing trend along IR1 > IR2 > IR3, in line with reduced urban influence downstream. TR2, though aligned in parallel with LR1, exhibited lower concentrations due to less urban input. TR1 showed the lowest detection frequency and concentrations, indicating no urban impact. Regarding seasons, winter had the highest concentrations for the year 2024, followed by spring, autumn, and summer (for the year 2023, autumn > winter > summer > spring). ATM, CFC, TMP and SMX were strongly influenced by location ($p < 0.05$—0.001), while CFC also showed significant seasonal effects ($p < 0.001$). Notably, interaction effects (season × location) were significant for CFC, SMX and TMP, indicating that spatial differences in pharmaceutical concentrations were influenced by seasonal changes, including input rate or consumption, water flow rate or dilution, temperature and microbial activity [9, 13, 62]. In most of the cases the pharmaceutical concentrations in water were significantly affected by both season and location, confirming the combined impact of urban impact and environment conditions, such as changes in drug consumption as well as hydrological and degradation conditions, as similarly reported [14].

For sediments, location had a consistently significant effect on the distribution of most compounds (except SMX), including CBZ, NPX, IBU, AETM (2024), ATM, CFC, and TMP ($p < 0.05 - 0.001$), indicating strong site specific influence, potentially related to urban discharge input and site-specific conditions (pH, OC and metal content), especially for location LR1. Seasonal variation was also significant for spring compared to summer samples for several compounds, particularly CBZ (2024), NPX, IBU (2023), ATM, CFC, SMX (2024), and TMP, suggesting fluctuations in consumption (input rate) and possibly environmental factors such as precipitation and temperature. Notably, the interaction between season and location was significant for CBZ, AETM, and CFC in at least one of the study years, pointing to complex spatial seasonal dynamics. The total pharmaceutical concentration, similarly, as water samples, showed strong effects of both season and location ($p < 0.001$), indicating that both natural and human factors substantially affect contaminant distribution in the Ishmi River basin.

Conclusions

The selected pharmaceuticals were detected at all locations within the Ishmi River basin, with higher concentrations at urban impacted locations. In water, CAFF,

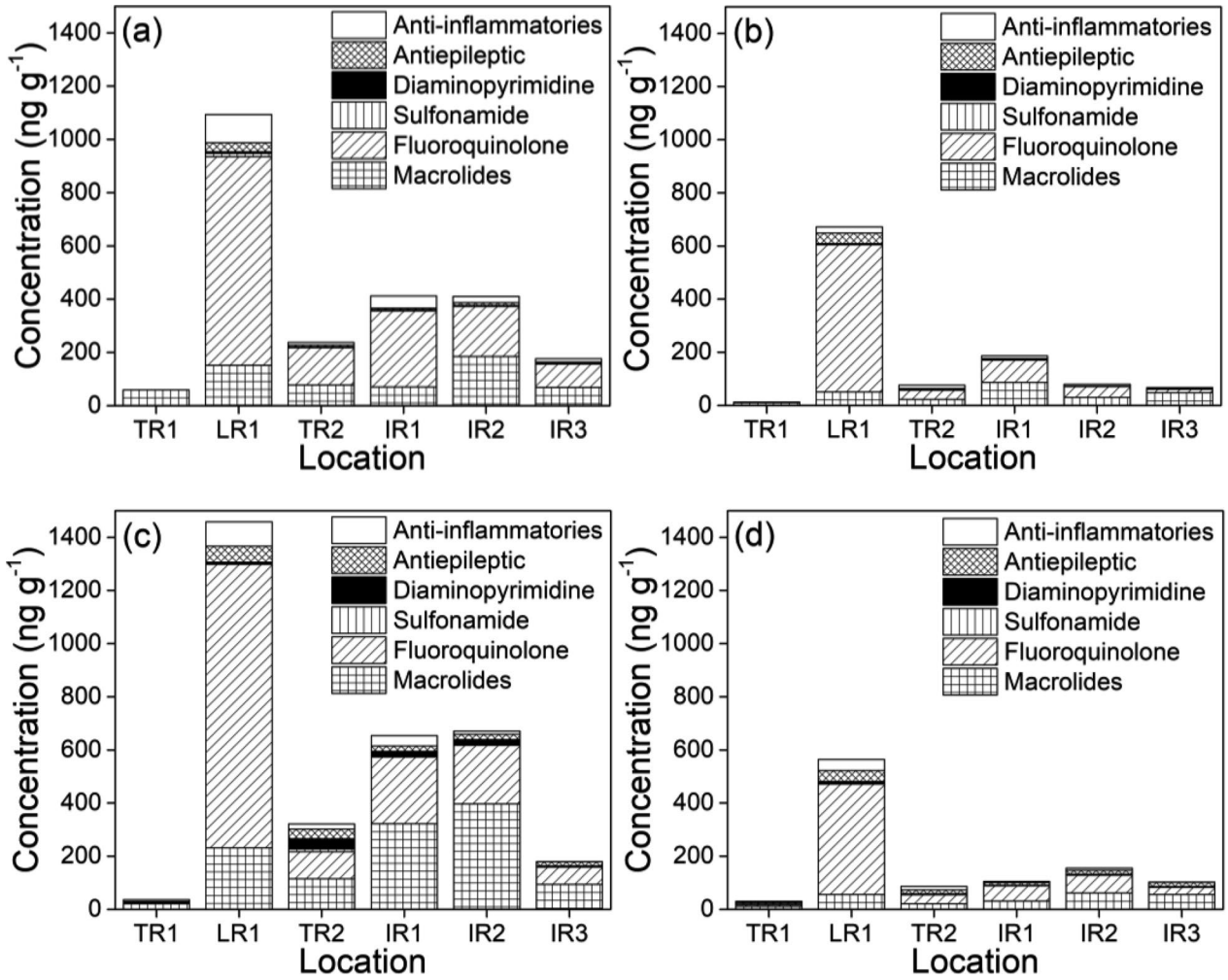

Fig. 6 Seasonal and spatial variations of selected pharmaceuticals in sediments of the Ishmi River basin for (**a**) spring and (**b**) summer of the year 2023; and (**c**) spring and (**d**) summer of the year 2024

IBU, NPX, and CFC were mostly detected, especially during winter, reflecting seasonal usage and environmental factors influence. In sediments, CFC and ATM dominated, with higher concentrations in spring, particularly at locations with low pH values and high organic carbon content. In situ partition coefficient like K_d and K_{oc} were derived from sediment and water concentrations of some frequently detected pharmaceuticals and the influence of intrinsic properties of the compounds and extrinsic environmental conditions were assessed by regression analysis. These analysis revealed that partitioning behavior was significantly influenced by compound-specific properties such as D_{ow}, as well as sediment-specific properties. These findings highlight the role of both intrinsic and extrinsic factors in controlling pharmaceutical distribution between water and sediment.

Abbreviations

CAFF	Caffeine
CBZ	Carbamazepine
NPX	Naproxen
IBU	Ibuprofen
DCF	Diclofenac
AETM	Anhydro-erythromycin
ATM	Azithromycin
CMC	Clindamycin
CFC	Ciprofloxacin
ETM	Erythromycin
SMX	Sulfamethoxazole
TMP	Trimethoprim
NSAIDs	Non-steroidal anti-inflammatory drugs
EU	European Union
TR1	Tirana river 1
LR1	Lana river 1
TR2	Tirana river 2
IR1	Ishmi river 1
IR2	Ishmi river 2
IR3	Ishmi river 3
C_s	Concentration in the sediment phase
C_w	Concentration in the water phase

K_d	Sediment–water partition coefficient
f_{oc}	Fraction of organic carbon
K_{oc}	Organic carbon-normalized partition coefficient
pK_a	Acid dissociation constant
K_{ow}	*n*-Octanol–water partition coefficient
D_{ow}	PH-dependent *n*-octanol–water partition coefficient
IC	Inorganic carbon
OC	Organic carbon
$CaCO_3$	Carbonates
TOC	Total carbon
SPE	Solid phase extraction
ACN	Acetonitrile
EDTA	Ethylenediaminetetraacetic acid disodium salt dihydrate
ANOVA	Analysis of variance
RMSE	Root mean square error
MW	Molecular weight

Supplementary Information

The online version contains supplementary material available at https://doi.org/10.1186/s12302-025-01264-w.

Supplementary file 1.

Acknowledgements
We acknowledge the support of Deutsche Bundesstiftung Umwelt (DBU), Germany, and the Erasmus+ program for the support of the research fellowships to A Peqini. Also, we acknowledge the support of E Müller and E Schneidenwind, J Junck, and A P Heinrich, iFZ, JLU Giessen, for technical assistance with HPLC and characterization of sediments.

Author contributions
AP executed the experiments, carried out the investigation and data curation, performed formal analysis, developed methodology, validated results, and prepared the initial draft. He was also responsible for resource collection (water and sediment sampling) and securing funding. BJH contributed to conceptualization, methodology development, data analysis, and validation. He also provided software support and was actively involved in reviewing and editing the manuscript. FB contributed to conceptualization and methodology, supervised the work, supported funding acquisition, and assisted in reviewing and editing the manuscript. RAD was involved in conceptualization, methodology, and validation, provided resources, supervised the research, administered the project, supported funding acquisition, and contributed to reviewing and editing the manuscript.

Funding
Open Access funding enabled and organized by Projekt DEAL

Data availability
All data generated or analysed during this study are included in this published article [and its supplementary information files].

Declarations

Ethics approval and consent to participate
Not applicable.

Consent for publication
Not applicable.

Competing interests
The authors declare no competing interests.

Received: 29 August 2025 Accepted: 30 October 2025
Published: 24 November 2025

References

1. Al-Khazrajy OSA, Boxall ABA (2016) Impacts of compound properties and sediment characteristics on the sorption behaviour of pharmaceuticals in aquatic systems. J Hazard Mater 317:198–209
2. Ashfaq M, Li Y, Rehman MSU, Zubair M, Mustafa G, Nazar MF, Yu CP, Sun Q (2019) Occurrence, spatial variation and risk assessment of pharmaceuticals and personal care products in urban wastewater, canal surface water, and their sediments: a case study of Lahore, Pakistan. Sci Total Environ 688:653–663
3. Bavumiragira JP, Ge J, Yin H (2022) Fate and transport of pharmaceuticals in water systems: a processes review. Sci Total Environ 823:153635
4. Borgnino L, Garcia MG, del Hidalgo MV, Avena M, De Pauli CP, Blesa MA, Depetris PJ (2009) Modeling the acid-base surface properties of aquatic sediments. Aquat Geochem 16:279–291
5. Carmona E, Andreu V, Pico Y (2014) Occurrence of acidic pharmaceuticals and personal care products in Turia River Basin: from waste to drinking water. Sci Total Environ 484:53–63
6. Chakraborty P, Mukhopadhyay M, Sampath S, Ramaswamy BR, Katsoyiannis A, Cincinelli A, Snow D (2019) Organic micropollutants in the surface riverine sediment along the lower stretch of the transboundary river Ganga: occurrences, sources and ecological risk assessment. Environ Pollut 249:1071–1080
7. Chen K, Zhou JL (2014) Occurrence and behavior of antibiotics in water and sediments from the Huangpu River, Shanghai, China. Chemosphere 95:604–612
8. Chen KL, Liu LC, Chen WR (2017) Adsorption of sulfamethoxazole and sulfapyridine antibiotics in high organic content soils. Environ Pollut 231:1163–1171
9. Da Silva BF, Jelic A, Lopez-Serna R, Mozeto AA, Petrovic M, Barcelo D (2011) Occurrence and distribution of pharmaceuticals in surface water, suspended solids and sediments of the Ebro river basin, Spain. Chemosphere 85:1331–1339
10. Dalkmann P, Broszat M, Siebe C, Willaschek E, Sakinc T, Huebner J, Amelung W, Grohmann E, Siemens J (2012) Accumulation of pharmaceuticals, Enterococcus, and resistance genes in soils irrigated with wastewater for zero to 100 years in central Mexico. PLoS ONE 7:e45397
11. de Souza RC, Godoy AA, Kummrow F, Dos Santos TL, Brandao CJ, Pinto E (2021) Occurrence of caffeine, fluoxetine, bezafibrate and levothyroxine in surface freshwater of Sao Paulo State (Brazil) and risk assessment for aquatic life protection. Environ Sci Pollut Res Int 28:20751–20761
12. Deng X, Jiang Y, Ma Z, Nan Z, Liang X, Wang G (2022) Sorption properties and mechanisms of erythromycin and ampicillin in loess soil: Roles of pH, ionic strength, and temperature. Chem Eng J 434:134694
13. Dong D, Zhang L, Liu S, Guo Z, Hua X (2016) Antibiotics in water and sediments from Liao River in Jilin Province, China: occurrence, distribution, and risk assessment. Environ Earth Sci. https://doi.org/10.1007/s12665-016-6008-4
14. Ebele AJ, Oluseyi T, Drage DS, Harrad S, Abou-Elwafa Abdallah M (2020) Occurrence, seasonal variation and human exposure to pharmaceuticals and personal care products in surface water, groundwater and drinking water in Lagos State, Nigeria. Emerg Contam 6:124–132
15. Feo ML, Bagnati R, Passoni A, Riva F, Salvagio Manta D, Sprovieri M, Traina A, Zuccato E, Castiglioni S (2020) Pharmaceuticals and other contaminants in waters and sediments from Augusta Bay (southern Italy). Sci Total Environ 739:139827
16. Gonzalez Pena OI, Lopez Zavala MÁ, Cabral Ruelas H (2021) Pharmaceuticals market, consumption trends and disease incidence are not driving the pharmaceutical research on water and wastewater. Int J Environ Res Public Health. https://doi.org/10.3390/ijerph18052532
17. Heyde BJ, Braun M, Soufi L, Lüneberg K, Gallego S, Amelung W, Axtmann K, Bierbaum G, Glaeser SP, Grohmann E, Arredondo-Hernández R, Mulder I, Pulami D, Smalla K, Zarfl C, Siebe C, Siemens J (2025) Transition from irrigation with untreated wastewater to treated wastewater and associated benefits and risks. NPJ Clean Water. https://doi.org/10.1038/s41545-025-00438-6

18. Hu Y, Yan X, Shen Y, Di M, Wang J (2018) Antibiotics in surface water and sediments from Hanjiang River, Central China: occurrence, behavior and risk assessment. Ecotoxicol Environ Saf 157:150–158
19. Jia J, Guan Y, Cheng M, Chen H, He J, Wang S, Wang Z (2018) Occurrence and distribution of antibiotics and antibiotic resistance genes in Ba River, China. Sci Total Environ 642:1136–1144
20. Kairigo P, Ngumba E, Sundberg L-R, Gachanja A, Tuhkanen T (2020) Contamination of surface water and river sediments by antibiotic and antiretroviral drug cocktails in low and middle-income countries: occurrence, risk and mitigation strategies. Water 12:1376
21. Kodesova R, Grabic R, Kocarek M, Klement A, Golovko O, Fer M, Nikodem A, Jaksik O (2015) Pharmaceuticals' sorptions relative to properties of thirteen different soils. Sci Total Environ 511:435–443
22. Kondor AC, Molnar E, Jakab G, Vancsik A, Filep T, Szeberenyi J, Szabo L, Maasz G, Pirger Z, Weiperth A, Ferincz A, Staszny A, Dobosy P, Horvathne Kiss K, Hatvani IG, Szalai Z (2022) Pharmaceuticals in water and sediment of small streams under the pressure of urbanization: concentrations, interactions, and risks. Sci Total Environ 808:152160
23. Kong W, Wang W, Jiang Y, Wang G, Ma F, Wu Y (2024) Sorption of ciprofloxacin and enrofloxacin on alkaline cropland soil in semiarid regions: roles of pH, ionic strength, and ion type. J Environ Manage 365:121565
24. Korekar G, Kumar A, Ugale C (2020) Occurrence, fate, persistence and remediation of caffeine: a review. Environ Sci Pollut Res Int 27:34715–34733
25. Kucharski D, Nalecz-Jawecki G, Drzewicz P, Skowronek A, Mianowicz K, Strzelecka A, Giebultowicz J (2022) The assessment of environmental risk related to the occurrence of pharmaceuticals in bottom sediments of the Odra River estuary (SW Baltic Sea). Sci Total Environ 828:154446
26. Kümmerer K (2009) The presence of pharmaceuticals in the environment due to human use–present knowledge and future challenges. J Environ Manage 90:2354–2366
27. Li J, Li W, Liu K, Guo Y, Ding C, Han J, Li P (2022) Global review of macrolide antibiotics in the aquatic environment: sources, occurrence, fate, ecotoxicity, and risk assessment. J Hazard Mater 439:129628
28. Li J, Zhang H (2017) Factors influencing adsorption and desorption of trimethoprim on marine sediments: mechanisms and kinetics. Environ Sci Pollut Res Int 24:21929–21937
29. Li S, Zhang R, Hu J, Shi W, Kuang Y, Guo X, Sun W (2019) Occurrence and removal of antibiotics and antibiotic resistance genes in natural and constructed riverine wetlands in Beijing, China. Sci Total Environ 664:546–553
30. Li WC (2014) Occurrence, sources, and fate of pharmaceuticals in aquatic environment and soil. Environ Pollut 187:193–201
31. Liu Z, Delgado-Moreno L, Lu Z, Zhang S, He Y, Gu X, Chen Z, Ye Q, Gan J, Wang W (2019) Inhibitory effects of dissolved organic matter on erythromycin bioavailability and possible mechanisms. J Hazard Mater 375:255–263
32. Maoz A, Chefetz B (2010) Sorption of the pharmaceuticals carbamazepine and naproxen to dissolved organic matter: role of structural fractions. Water Res 44:981–989
33. Martin J, Camacho-Munoz D, Santos JL, Aparicio I, Alonso E (2012) Occurrence of pharmaceutical compounds in wastewater and sludge from wastewater treatment plants: removal and ecotoxicological impact of wastewater discharges and sludge disposal. J Hazard Mater 239–240:40–47
34. Martin J, Santos JL, Aparicio I, Alonso E (2010) Multi-residue method for the analysis of pharmaceutical compounds in sewage sludge, compost and sediments by sonication-assisted extraction and LC determination. J Sep Sci 33:1760–1766
35. Mirzaei R, Yunesian M, Nasseri S, Gholami M, Jalilzadeh E, Shoeibi S, Mesdaghinia A (2018) Occurrence and fate of most prescribed antibiotics in different water environments of Tehran. Iran Sci Total Environ 619–620:446–459
36. Nguyen Dang Giang C, Sebesvari Z, Renaud F, Rosendahl I, Hoang Minh Q, Amelung W (2015) Occurrence and dissipation of the antibiotics sulfamethoxazole, sulfadiazine, trimethoprim, and enrofloxacin in the Mekong Delta, Vietnam. PLoS ONE 10:e0131855
37. Paiga P, Ramos S, Jorge S, Silva JG, Delerue-Matos C (2019) Monitoring survey of caffeine in surface waters (Lis River) and wastewaters located at Leiria Town in Portugal. Environ Sci Pollut Res Int 26:33440–33450
38. Paiga P, Santos L, Ramos S, Jorge S, Silva JG, Delerue-Matos C (2016) Presence of pharmaceuticals in the Lis river (Portugal): sources, fate and seasonal variation. Sci Total Environ 573:164–177
39. Patrolecco L, Ademollo N, Grenni P, Tolomei A, Barra Caracciolo A, Capri S (2013) Simultaneous determination of human pharmaceuticals in water samples by solid phase extraction and HPLC with UV-fluorescence detection. Microchem J 107:165–171
40. Perez RA, Albero B, Ferriz M, Tadeo JL (2017) Analysis of macrolide antibiotics in water by magnetic solid-phase extraction and liquid chromatography-tandem mass spectrometry. J Pharm Biomed Anal 146:79–85
41. Reyes CM, Cornelis MC (2018) Caffeine in the diet: country-level consumption and guidelines. Nutrients. https://doi.org/10.3390/nu10111772
42. Rodriguez-Mozaz S, Vaz-Moreira I, Varela Della Giustina S, Llorca M, Barcelo D, Schubert S, Berendonk TU, Michael-Kordatou I, Fatta-Kassinos D, Martinez JL, Elpers C, Henriques I, Jaeger T, Schwartz T, Paulshus E, O'Sullivan K, Parnanen KMM, Virta M, Do TT, Walsh F, Manaia CM (2020) Antibiotic residues in final effluents of European wastewater treatment plants and their impact on the aquatic environment. Environ Int 140:105733
43. Röhricht M, Krisam J, Weise U, Kraus UR, Düring R-A (2009) Elimination of carbamazepine, diclofenac and naproxen from treated wastewater by nanofiltration. CLEAN - Soil, Air, Water 37:638–641
44. Royano S, Navarro I, Torre A, Martinez MA (2024) Investigating the presence, distribution and risk of pharmaceutically active compounds (PhACs) in wastewater treatment plants, river sediments and fish. Chemosphere 368:143759
45. Schmidtova Z, Kodesova R, Grabicova K, Kocarek M, Fer M, Svecova H, Klement A, Nikodem A, Grabic R (2020) Competitive and synergic sorption of carbamazepine, citalopram, clindamycin, fexofenadine, irbesartan and sulfamethoxazole in seven soils. J Contam Hydrol 234:103680
46. Senta I, Terzic S, Ahel M (2021) Analysis and occurrence of macrolide residues in stream sediments and underlying alluvial aquifer downstream from a pharmaceutical plant. Environ Pollut 273:116433
47. Sung-Chul K, Kenneth C (2007) Temporal and spatial trends in the occurrence of human and veterinary antibiotics in aqueous and river sediment matrices. Environ Sci Technol 41:50–57
48. Svahn O, Bjorklund E (2015) Describing sorption of pharmaceuticals to lake and river sediments, and sewage sludge from UNESCO biosphere reserve Kristianstads Vattenrike by chromatographic asymmetry factors and recovery measurements. J Chromatogr A 1415:73–82
49. Tang J, Wang S, Fan J, Long S, Wang L, Tang C, Tam NF, Yang Y (2019) Predicting distribution coefficients for antibiotics in a river water-sediment using quantitative models based on their spatiotemporal variations. Sci Total Environ 655:1301–1310
50. Thiele-Bruhn S (2003) Pharmaceutical antibiotic compounds in soils – a review. J Plant Nutr Soil Sci 166:145–167
51. Valcarcel Y, Gonzalez Alonso S, Rodriguez-Gil JL, Gil A, Catala M (2011) Detection of pharmaceutically active compounds in the rivers and tap water of the Madrid Region (Spain) and potential ecotoxicological risk. Chemosphere 84:1336–1348
52. Van Doorslaer X, Dewulf J, Van Langenhove H, Demeestere K (2014) Fluoroquinolone antibiotics: an emerging class of environmental micropollutants. Sci Total Environ 500–501:250–269
53. Vasudevan D, Bruland GL, Torrance BS, Upchurch VG, MacKay AA (2009) pH-dependent ciprofloxacin sorption to soils: interaction mechanisms and soil factors influencing sorption. Geoderma 151:68–76
54. Vazquez-Roig P, Andreu V, Blasco C, Pico Y (2012) Risk assessment on the presence of pharmaceuticals in sediments, soils and waters of the Pego-Oliva Marshlands (Valencia, eastern Spain). Sci Total Environ 440:24–32
55. Vermillion Maier ML, Tjeerdema RS (2018) Azithromycin sorption and biodegradation in a simulated California river system. Chemosphere 190:471–480
56. Vulava VM, Cory WC, Murphey VL, Ulmer CZ (2016) Sorption, photodegradation, and chemical transformation of naproxen and ibuprofen in soils and water. Sci Total Environ 565:1063–1070
57. Wilkinson JL, Boxall ABA, Kolpin DW, Leung KMY, Lai RWS, Galbán-Malagón C et al (2022) Pharmaceutical pollution of the world's rivers. Proc Natl Acad Sci U S A 119:e21139
58. Ying G-G, Zhao J-L, Zhou L-J, Liu S (2013) Fate and Occurrence of Pharmaceuticals in the Aquatic Environment (Surface Water and Sediment). 62: 453-557

59. Zhao S, Liu X, Cheng D, Liu G, Liang B, Cui B, Bai J (2016) Temporal-spatial variation and partitioning prediction of antibiotics in surface water and sediments from the intertidal zones of the Yellow River Delta, China. Sci Total Environ 569–570:1350–1358
60. Zhou H, Wu C, Huang X, Gao M, Wen X, Tsuno H, Tanaka H (2010) Occurrence of selected pharmaceuticals and caffeine in sewage treatment plants and receiving rivers in Beijing, China. Water Environ Res 82:2239–2248
61. Zhou J, Broodbank N (2014) Sediment-water interactions of pharmaceutical residues in the river environment. Water Res 48:61–70
62. Zhou LJ, Ying GG, Zhao JL, Yang JF, Wang L, Yang B, Liu S (2011) Trends in the occurrence of human and veterinary antibiotics in the sediments of the Yellow River, Hai River and Liao River in northern China. Environ Pollut 159:1877–1885

Publisher's Note